

Exceptional stationary state in a dephasing many-body open quantum system

Alice Marché,^{1,*} Gianluca Morettini,^{1,*} Leonardo Mazza,^{1,2} Lorenzo Gotta,³ and Luca Capizzi¹

¹*Université Paris-Saclay, CNRS, LPTMS, 91405, Orsay, France.*

²*Institut Universitaire de France, 75005 Paris, France.*

³*Department of Quantum Matter Physics, University of Geneva, 1211 Geneva, Switzerland.*

(Dated: 19th December 2024)

We study a dephasing many-body open quantum system that hosts, together with the infinite-temperature state, another additional stationary state. The latter is exceptional in many respects, as it is pure and retains memory of the initial condition, whereas any orthogonal state evolves towards the infinite-temperature state erasing any information on the initial state. We discuss the approach to stationarity of the model focusing in particular on the fate of interfaces between the two states; a simple classical model based on a membrane picture helps developing an effective hydrodynamic theory even if the dynamics does not feature any conserved quantity. The fact that the model reaches stationary properties on timescales that depend on the system size while the asymptotic decay rate is finite is duly highlighted. We point out the reasons for considering these exceptional stationary states as quantum many-body scars in the open system framework.

Introduction — The eigenstate thermalization hypothesis (ETH) stands as a cornerstone in condensed-matter physics, as it describes in simple and physical terms the emergence of thermal features in the late-time dynamics of closed quantum systems [1–5]. In the last years, the study of exceptional dynamics that escape thermalization by retaining memory of the initial conditions, has been identified as a primary mechanism for achieving the presence of rare eigenstates that violate the ETH, dubbed many-body quantum scars [6–10]. The broad goal of this article is to study a similar phenomenon in Markovian many-body open quantum systems (MBOQS) [11, 12], discussing in detail a specific dephasing model.

The late-time behaviour of Markovian MBOQS [13, 14], and particularly the study of the steady states of dephasing models, has recently attracted a great deal of attention [15–21]. In the absence of any strong symmetry [22, 23], one generically expects a unique stationary state that is progressively approached from any initial state, leading to the complete erasure of any information on the initial state. The behaviour resembles closely the ergodicity that always accompanies thermalization in closed systems. Whether a dephasing model could withstand also an exceptional stationary state showcasing the existence of peculiar initial conditions whose memory is retained notwithstanding the coupling to an external bath, is something that has not been discussed yet.

In this article we consider a dephasing model where an additional stationary state arises that is not protected by strong symmetries, and that plays the role of a scar in this MBOQS. Specifically, we study a one-dimensional model where both the fully-polarized pure state and the infinite-temperature (mixed) state are stationary: we show, with both analytical and numerical techniques, that these are

the only steady ones. The relaxation time of local observables is shown to be algebraically long in the system size, albeit a finite spectral gap in the Lindbladian is present; a similar observation has been pointed out in different contexts in Refs. [24–27]. To understand the mechanism underlying the dynamics, we develop a membrane picture that describes the fate of interfaces between the two steady states: their ballistic drift and diffusive fluctuations are uncovered, showcasing a hydrodynamic behaviour that is not associated to any local conserved quantity. Our work proposes a novel view on many-body quantum scars in MBOQS as *exceptional stationary states* that parallels the weak ETH violation associated to scars in the unitary context.

The model — We consider a one-dimensional spin-1/2 chain of length L whose density matrix ρ evolves according to the Lindblad master equation

$$\frac{d}{dt}\rho = \mathcal{L}[\rho] = -i[H, \rho] + \sum_j L_j \rho L_j^\dagger - \frac{1}{2}\{L_j^\dagger L_j, \rho\}, \quad (1)$$

with jump operators $L_j = \sqrt{\gamma}\sigma_j^z$ and Hamiltonian

$$H = \sum_j J [\sigma_j^+ \sigma_{j+1}^- + H.c.] + g [\sigma_j^x \pi_{j+1}^z + \pi_j^z \sigma_{j+1}^x], \quad (2)$$

where $\pi_j^\alpha = \mathbb{1} - \sigma_j^\alpha$, for $\alpha = x, y, z$. Here, J is the strength of the nearest-neighbor hopping term, while g multiplies the East-West Hamiltonian [28], according to which a spin can be flipped only when a neighboring spin is in a $|\downarrow\rangle$ state. The dissipation occurs at a rate γ and it is associated with the decay of coherence in the z -polarized basis; as such it is naturally interpreted as a *dephasing* process.

Stationary states — Strong symmetries, i.e. operators A that simultaneously satisfy both $[H, A] = 0$ and $[L_j, A] = 0$, generalize the usual notion of symmetry in isolated systems to the MBOQS framework [22, 23]. Using the fact that all jump operators are Hermitian,

* These authors contributed equally.

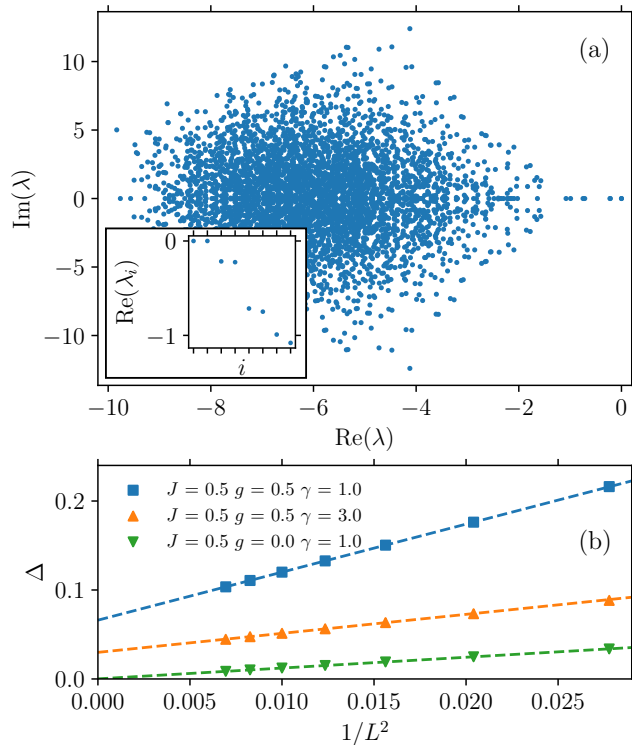


Figure 1. (a) Lindbladian spectrum for the following parameters: $[J, g, \gamma, L] = [0.5, 0.5, 1, 6]$. Inset: real parts of the eigenvalues the closest to zero labeled by the index i . (b) Lindbladian gap Δ as a function of $1/L^2$ for $L \in \{6, \dots, 12\}$. The results are compatible with a scaling $\Delta(L) = \Delta_0 + \Delta_1/L^2 + o(L^{-2})$. The three curves correspond to different sets of parameters: $[J, g, \gamma] = [0.5, 0.5, 1]$, $[0.5, 0.5, 3]$ or $[0.5, 0, 1]$. For both panels (a) and (b), open boundary conditions are considered.

namely $L_j = L_j^\dagger$, we can rewrite the Lindbladian as $\mathcal{L}[\rho] = -i[H, \rho] - \frac{1}{2} \sum_j [L_j, [L_j, \rho]]$ and get to the conclusion that any state ρ that is a strong symmetry, will also be stationary $\mathcal{L}[\rho] = 0$. The study of strong symmetries thus retains a special importance for this model.

Specifically, as it is always true when $L_j = L_j^\dagger$, the *infinite temperature state* $\rho_\infty = \mathbb{1}/\text{Tr}[\mathbb{1}]$ is stationary, that is $\mathcal{L}[\rho_\infty] = 0$. Instead, the magnetisation $\sum_j \sigma_j^z$ is not, in general, a strong symmetry and it evolves non-trivially during the open dynamics. Nonetheless, given the specific choice of Hamiltonian [28, 29] and dissipation in Eq. (2), the pure state $\rho_\uparrow = |\uparrow\rangle\langle\uparrow|$ associated with all spins aligned along the z axis, is stationary, as it constitutes a non-trivial strong symmetry of the model; in particular, the subspace generated by $|\uparrow\rangle$ is decoherence-free [30]. Note that the two states are not orthogonal according to the Hilbert-Schmidt scalar product $\langle\rho, \tau\rangle_{\text{HS}} := \text{Tr}[\rho^\dagger \tau]$ because $\langle\rho_\uparrow, \rho_\infty\rangle_{\text{HS}} = 2^{-L}$; hence it will be more useful in the following to consider $\rho'_\infty := (\mathbb{1} - \rho_\uparrow)/\text{Tr}[\mathbb{1} - \rho_\uparrow]$, whose local properties differ from those of ρ_∞ by a term that is exponentially small

in the system size but that is orthogonal to ρ_\uparrow .

No additional states are stationary. In order to prove this statement, we consider the Lindbladian \mathcal{L} , which is a linear non-Hermitian superoperator, and study its complex spectrum, plotted in Fig. 1(a), obtained with the exact-diagonalization (ED) of a spin chain of size $L = 6$. The calculation is performed with the open-source python-framework QuTiP [31, 32]. The inset shows that the eigenvalue $\lambda = 0$ is two-fold degenerate, and we have checked that the two associated eigenvectors can be identified with ρ_∞ and ρ_\uparrow . This feature is compatible with properties of the commutant algebra [20, 33–35] of the model, derived in the End Matter (EM) and detailed in the Supplemental Material (SM) [36], that encodes important information about the stationary states.

The numerics allows us also to conclude that the Lindbladian spectral gap, $\Delta = \min_{\lambda \neq 0} |\text{Re}[\lambda]|$ does not close with system size, and specifically that it has a large- L scaling $\Delta(L) \simeq \Delta_0 + \frac{\Delta_1}{L^2}$ with $\Delta_0 \neq 0$ whenever $g \neq 0$ [37]. The numerical scaling of $\Delta(L)$ is presented in Fig. 1(b) for sizes up to $L = 12$. We have observed that the specific value of Δ_0 depends on the choice of open versus periodic boundary conditions (see EM).

Dynamics — We argue that any initial pure state $|\psi\rangle$ that is orthogonal to $|\uparrow\rangle$ must relax eventually towards ρ'_∞ . The approach to ρ'_∞ can be quantified by the normalized Hilbert-Schmidt scalar product:

$$\theta'_\infty(t) := \frac{\text{Tr}[\rho'_\infty \rho(t)]}{\sqrt{\text{Tr}[\rho_\infty^2] \text{Tr}[\rho(t)^2]}}, \quad (3)$$

that generalizes the scalar product $|\langle\psi|\psi'\rangle|^2$ (which holds for pure states). Since ρ'_∞ and $\rho(t)$ are positive and Hermitian operators, $\theta'_\infty(t) \geq 0$. Moreover, by the Cauchy-Schwartz inequality $\theta'_\infty(t) \leq 1$ and $\theta'_\infty(t) = 1$ if and only if $\rho(t) \equiv \rho'_\infty$; in particular, whenever $\langle\psi|\uparrow\rangle = 0$, $\theta'_\infty(t)$ is expected to converge to 1 at sufficiently large time t .

We employ the ITensor julia library [38, 39] and develop a tensor-network representation of the density matrices ρ'_∞ and $\rho(t)$, where the latter is computed with an algorithm based on the time-dependent variational principle [40, 41] that integrates the dynamics (1); details are given in the EM. The scalar product $\theta'_\infty(t)$ has a natural interpretation in terms of tensor-network contractions and can be efficiently computed. This allows us to study chains of length $L = 40$, which would not have been possible with ED techniques (although we benchmarked our algorithm against ED for smaller system sizes).

Our results are plotted in Fig. 2(a) and demonstrate the time-evolution towards ρ'_∞ of three translationally-invariant initial states orthogonal to $|\uparrow\rangle$, namely the fully-polarized state $|\Downarrow\rangle$ with all spins in the $|\downarrow\rangle$ state, the antiferromagnetic Néel state $|\text{Néel}\rangle = |\uparrow\downarrow\uparrow\downarrow\uparrow\downarrow\dots\rangle$, and the state $|\uparrow\downarrow\downarrow\uparrow\uparrow\downarrow\downarrow\dots\rangle$. We also verified numerically the fact that $|\uparrow\rangle$ is stationary and retains $\theta'_\infty(t) = 0$ at all times.

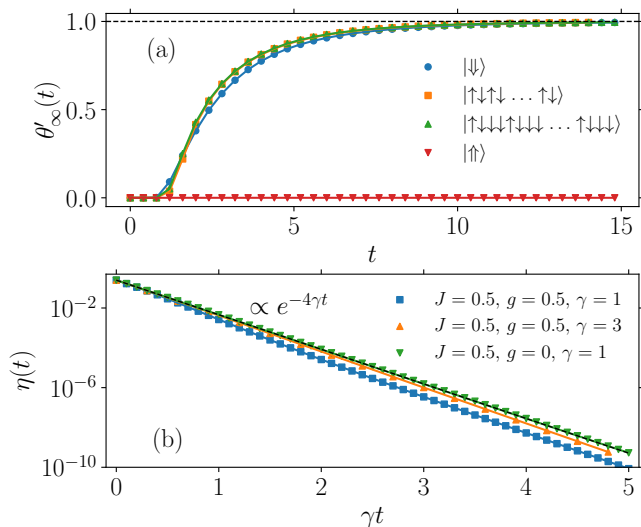


Figure 2. (a) Time-evolution of $\theta'_\infty(t)$ for the initial states $|\Downarrow\rangle$, $|\text{Néel}\rangle$, $|\uparrow\downarrow\downarrow\uparrow\downarrow\downarrow\dots\rangle$, and $|\uparrow\rangle$. The parameters are $[J, g, \gamma, L] = [0.5, 0.5, 1, 40]$. (b) Time-evolution of $\eta(t)$ for the initial state $|\uparrow\dots\uparrow\rangle$. We observe that the upper bound is saturated for $g = 0$.

These results highlight the separation of the Hilbert space into two disconnected subspaces. On the one hand, we have the state $|\uparrow\rangle$ and the associated subspace \mathcal{S}_\uparrow . On the other hand, the subspace \mathcal{T}_\uparrow , orthogonal to \mathcal{S}_\uparrow , is characterized by a total loss of information concerning the initial conditions, and an eventual relaxation toward the stationary state ρ'_∞ .

We now show that any coherence between the two subspaces \mathcal{T}_\uparrow and \mathcal{S}_\uparrow is lost exponentially in time by introducing the quantifier:

$$\eta(t) := \sum_{|\sigma\rangle \neq |\uparrow\rangle} |\langle \sigma | \rho(t) | \uparrow \rangle|^2, \quad (4)$$

where $\{|\sigma\rangle\}$ is a basis for the Hilbert space of the entire spin chain composed of states that are simultaneous eigenstates of all σ_j^z ; the sum is restricted over a basis of \mathcal{T}_\uparrow . With a few simple algebraic passages, we obtain the following suggestive rewriting: $\eta(t) = \langle \uparrow | \rho(t)^2 | \uparrow \rangle - \langle \uparrow | \rho(t) | \uparrow \rangle^2$, which proposes the simple interpretation of $\eta(t)$ as the variance of the operator $\rho(t)$ on the state $|\uparrow\rangle$, and proves that the definition of $\eta(t)$ is basis independent. By definition, $0 \leq \eta(t) \leq 1$.

In the EM, we detail a few algebraic passages that demonstrate the inequality $\frac{d}{dt}\eta(t) \leq -4\gamma\eta(t)$, and thus that $\eta(t) \leq \eta(0)e^{-4\gamma t}$, proving an exponential decay in time of the coherence between the two subspaces associated with the two different dynamics. We explicitly verified this prediction with our ITensors numerics for a system of length $L = 40$ initialized in the state $|\uparrow\dots\uparrow\rangle$. Our results are reported in Fig. 2(b) and satisfy the exponential bound we just derived.

Open-system quantum many-body scars — The results presented so far motivate the interpretation of the Lindblad model in Eq. (1) as an *open-system generalization of quantum many-body scars*, and specifically of isolated scars [28, 29]. In the Hamiltonian evolution framework, the remarkable property of a quantum many-body scar is the fact that it exceptionally escapes thermalization, namely that it maintains information on the initial condition [7–10]. For our model, it is not possible to speak of thermalization in a strict sense, as the MBOQS dynamics we are focusing on does not conserve energy, and rather the system relaxes generically towards the infinite temperature state, without the possibility of considering different temperatures. Yet, as it happens in the unitary framework, there is a competition between (i) a generic ergodic behaviour that erases information on the initial state and produces an incoherent mixture of any state in \mathcal{T}_\uparrow , and (ii) an exceptional one in \mathcal{S}_\uparrow , that only pertains to a unique well-defined initial state. According to us, the analogy with scars is meaningful.

Definitions of quantum many-body scars in MBOQS have already appeared in the literature. In Ref. [42] it has been shown that scars can be stationary states of specific models, but no competition between generic and exceptional dynamics is present there, so that the model is very close to the literature on dissipative quantum state engineering. In Ref. [43] a family of stationary states in Lindblad models supporting a strong symmetry are identified and admit a simple tensor-network representation; it is not obvious to us that these models feature a competition between generic and exceptional dynamics, due to the presence of the strong symmetry. Our work instead wants to insist exactly on that point. For other works on the general subject of non-ergodicity and the retain of quantum coherence in open systems, see Refs. [44–46].

Hydrodynamics of the interface — We conclude by discussing initial states that are spatially inhomogeneous and can be interpreted as interfaces of the two stationary states that we have identified. We consider the simplest, that has on the left half-chain $j < 0$ the infinite-temperature state and on the right half-chain $j \geq 0$ the scar: with a slight abuse of notation, we denote it as $\rho(0) = \rho_\infty \otimes \rho_\uparrow$. According to the theory presented above, this state should evolve at late time towards the state ρ_∞ , apart from negligible corrections that scale as 2^{-L} ; it thus constitutes an excellent playground for studying how an isolated scar affects the thermalization dynamics in a MBOQS.

The numerical results obtained with the use of MPOs and the ITensor library are presented in Fig. 3. The plot of the local magnetization $\langle \sigma_j^z(t) \rangle := \text{Tr}[\sigma_j^z \rho(t)]$ shows the progressive melting of the fully-polarized scar, a phenomenology compatible with the expectation that this initial state should thermalize. The interface drifts towards the right and as time flows it smooths out, even if it is initially sharp. Our goal is to present a descrip-

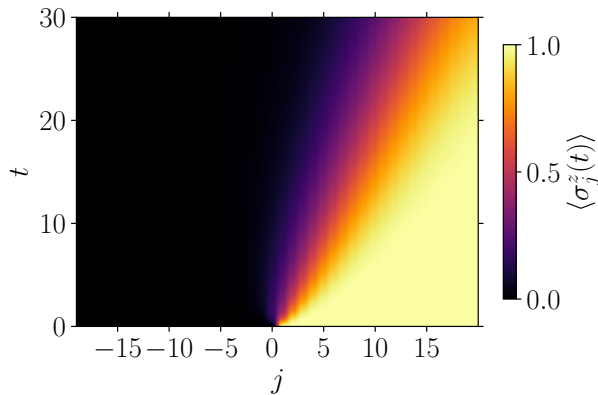


Figure 3. Magnetization profile $\langle \sigma_j^z(t) \rangle$ as a function of j and t . The initial state is obtained by joining the infinite-temperature state, with support $j \in [-L/2 + 1, 0]$, and the full-aligned up state along the z -axis elsewhere. The evolution is performed for the model in Eqs. (1) with the following parameters: $[J, g, \gamma, L] = [0.5, 0.5, 1, 40]$.

tion of the interface dynamics in Fig. 3 and to develop a suitable hydrodynamic theory even if the system does not support *local* strong symmetries: we employ a *membrane picture* [47, 48] to describe the fluctuating dynamics of the interface separating the infinite temperature state and the scar respectively.

We are able to pinpoint analytically this picture in the large- γ limit of the dynamics (1) using the second-order perturbation theory for $g/\gamma, J/\gamma \ll 1$ introduced in Ref. [17] for dephasing models. It is based on an effective Lindbladian \mathcal{L}_{eff} that acts onto the states $\rho_\sigma = |\sigma\rangle\langle\sigma|$, which are easily proven to be the only stationary states in the limit $g, J = 0$ and thus determine the late-time dynamics $t \gg \gamma^{-1}$ of the model for $g/\gamma, J/\gamma \ll 1$.

The action of \mathcal{L}_{eff} onto a density matrix $\rho(t) = \sum_\sigma p_\sigma(t) |\sigma\rangle\langle\sigma|$, is most easily described using the Doi-Peliti formalism that represents the density matrix $\rho(t)$ as a vector $|\rho(t)\rangle = \sum_\sigma p_\sigma(t) |\sigma\rangle$ that satisfies the unconventional normalization condition $\sum_\sigma p_\sigma = 1$ [49, 50]. The Lindblad dynamics $\frac{d}{dt}|\rho(t)\rangle = \mathcal{L}_{\text{eff}}|\rho(t)\rangle$ is translated into the form $\frac{d}{dt}|\rho(t)\rangle = -W|\rho(t)\rangle$ with the Markov generator (see EM and SM [36])

$$W = -\frac{J^2}{4\gamma} \sum_j (\sigma_j^x \sigma_{j+1}^x + \sigma_j^y \sigma_{j+1}^y + \sigma_j^z \sigma_{j+1}^z - 1) + 2\frac{g^2}{\gamma} \sum_j (\pi_j^x \pi_{j+1}^z + \pi_{j+1}^x \pi_j^z + \pi_{j-1}^z \pi_j^x \pi_{j+1}^z). \quad (5)$$

Since the dynamics induced by W cannot be determined analytically, we propose a simplified Markov generator for which the interface dynamics can be solved analytically: $\tilde{W} = W - 2(g^2/\gamma) \sum_j \pi_{j-1}^z \pi_j^x \pi_{j+1}^z$ so that the terms coupling three sites are discarded. We also make a specific choice of the parameters, namely $J^2/4\gamma = 1/6$

and $2g^2/\gamma = 1/6$: this allows us to provide rigorous estimates for the spectral gap (reported in the SM [36]) and exact calculations for the interface dynamics.

We introduce the vector $|\bullet\rangle = \frac{1}{2}(|\uparrow\rangle + |\downarrow\rangle)$, namely the local infinite temperature state, and we define the state $|x\rangle \equiv |\bullet \dots \bullet \uparrow \dots \uparrow\rangle_x$, representing an interface between the positions x and $x+1$. The states $|x\rangle$ are the essence of the membrane picture. By explicit computation, it is possible to show that $\tilde{W}|x\rangle = |x\rangle - \frac{2}{3}|x+1\rangle - \frac{1}{3}|x-1\rangle$, and therefore the space of single domain-wall states is closed under Markov dynamics; in particular, the evolution reduces to a one-dimensional Brownian motion with drift on the lattice, which can be solved exactly using the Fourier transform. The explicit solution is $|\rho(t)\rangle = e^{-\tilde{W}t}|x=0\rangle = \sum_x p(x,t)|x\rangle$ with $p(x,t) \equiv \int_{-\pi}^{\pi} \frac{dk}{2\pi} \exp(-\varepsilon(k)t + ikx)$, where $\varepsilon(k) = 1 - \cos(k) + \frac{i}{3} \sin k$. Here, $p(x,t)$ is the probability distribution of the domain-wall position; in the large t limit, we approximate it as

$$p(x,t) \simeq \frac{1}{\sqrt{2\pi\mathcal{D}t}} \exp\left(-\frac{(x-vt)^2}{2\mathcal{D}t}\right). \quad (6)$$

where $v = 1/3$ and $\mathcal{D} = 1$, the *drift velocity* and the *diffusion constant* respectively, are defined by the small k expansion $\varepsilon(k) \simeq ivk + \frac{1}{2}\mathcal{D}k^2 + O(k^3)$.

We now discuss the time evolution of the expectation value of σ_j^z plotted in Fig. 3, which is a local classical observable (namely, it is diagonal in the $\{|\sigma\rangle\}$ basis). The expectation value of the local magnetization operator σ_j^z is particularly simple, $\langle \sigma_j^z(t) \rangle = \sum_{j' < j} p(j', t)$; in the large-scale hydrodynamic limit where the discrete lattice site j is replaced by a continuous variable x , it can be approximated by

$$\langle \sigma^z(x,t) \rangle \simeq \int_{-\infty}^{\frac{x-vt}{\sqrt{\mathcal{D}t}}} \frac{du}{\sqrt{2\pi}} \exp\left(-\frac{u^2}{2}\right), \quad (7)$$

and it is thus proportional to the Error function.

In Fig. 4 we show that the membrane picture gives an accurate description of the interface hydrodynamics. By collapsing the data presented in Fig. 3 against the rescaled variable $(x-vt)/\sqrt{\mathcal{D}t}$, we show that the interface is actually evolving via a diffusive broadening with drift, even if the analytical picture was developed in the large dissipation limit. The values of v and \mathcal{D} employed in the figure have been fitted.

Late-time asymptotics and spectral gap We conclude by mentioning an interesting feature of our model. In the first part of the letter, we showed that the Lindbladian gap is finite in the thermodynamic limit. In general, this should be interpreted as the existence of a finite asymptotic decoherence rate, and thus of a typical time-scale $\tau_0 \sim 1/\Delta_0$ that does not depend on the system size and that gives an upper bound to the time that is necessary for the system to reach stationarity. Our

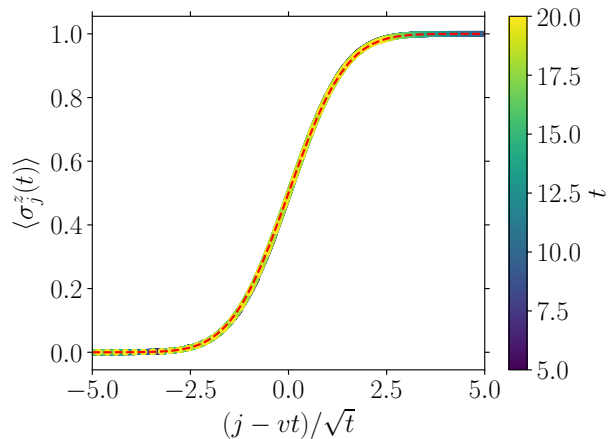


Figure 4. Profile of the magnetization shown in Fig. 3 as a function of the scaling variable $(j - vt)/\sqrt{t}$. The rescaled data collapse onto the universal function described by Eq. (7), represented by the red dashed line. The velocity v is determined by interpolating numerically, at each time t , the position x where the profile satisfies $\langle \sigma_j^z(t) \rangle = 0.5$. The diffusion constant \mathcal{D} is a fitting parameter. Here, $v \simeq 0.453$ and $\mathcal{D} \simeq 1.33$. Parameters used: $[J, g, \gamma, L] = [0.5, 0.5, 1, 40]$.

numerics in Fig. 3 and the membrane analytical picture, instead, show a very different behaviour: the interface state displays a thermalization dynamics whose timescale must necessarily grow with the size of the system, as the drift velocity and the diffusion constant are finite in the thermodynamic limit. This result suggests that the identification of the *bona fide* asymptotic decay rate in a MBOQS requires a careful study not only of the Lindbladian spectral properties, but also of the size-dependence of the decomposition of initial states onto the eigenvectors of the Lindbladian [24–27].

Conclusions — We have discussed a MBOQS dephasing model with an exceptional and pure stationary state $|\uparrow\rangle$ that retains the memory of the initial condition while any other initial state relaxes towards the infinite-temperature state ρ'_∞ . We have employed this model to stress a viewpoint on quantum many-body scars in open systems based on the juxtaposition of generic and exceptional dynamics. We have shown that the presence of the scar induces in the model a diffusive phenomenon that is not linked to local strong symmetries. The work opens the path toward the study of dynamics in the presence of exceptional stationary states, the universal features of the long-time dynamics, and their relation with the spectral properties of the Lindbladian [12, 51, 52].

Acknowledgements — We are indebted to M. Fagotti for enlightening discussions on this and related projects. We are grateful to M. C. Bañuls, B. Buca, H. Katsura, M. Schirò and L. Zadnik for several discussions. L.M. thanks also R. Fazio and J. Keeling for uncountable

discussions on many-body open quantum systems. L.C. acknowledges support from ERC Starting Grant 805252 LoCoMacro. This work has benefited from a State grant as part of France 2030 (QuantEdu-France), bearing the reference ANR-22-CMAS-0001 (G.M.), and is part of HQI (www.hqi.fr) initiative, supported by France 2030 under the French National Research Agency award number ANR-22-PNCQ-0002 (L.M.). This work is supported by the ANR project LOQUST ANR-23-CE47-0006-02 (L.M. and L.C.). This work was carried out in the framework of the joint Ph.D. program between the CNRS and the University of Tokyo (A.M.). This work was supported by the Swiss National Science Foundation under Division II grant 200020-219400 (L.G.).

End Matter

Commutant algebra — We discuss the properties of the commutant algebra (reviewed in [33, 34]) associated with the model in Eq. (1) of the main text. Such analysis is particularly useful for open quantum systems, as shown in Ref. [20], since it allows us to identify in general a set of (both local and non-local) symmetries associated with the terms appearing in the Lindbladian (for a generic choice of the couplings). For instance, given the Hamiltonian $H = \sum_j h_j$ and the local dissipators L_j , one defines the commutant algebra \mathcal{C}

$$\mathcal{C} := \{\mathcal{O} \mid [\mathcal{O}, h_j] = [\mathcal{O}, L_j] = [\mathcal{O}, L_j^\dagger] = 0 \forall j\}. \quad (8)$$

We observe that the dissipators of (1) are hermitian, $L_j^\dagger = L_j$, and both $\mathbb{1}$ and $|\uparrow\rangle\langle\uparrow|$ belong to \mathcal{C} . Specifically, one can show that $\mathcal{C} = \text{Span}\{\mathbb{1}, |\uparrow\rangle\langle\uparrow|\}$, meaning that these operators generate the entire commutant algebra. We sketch the proof below:

- Since we are interested in $g, J \neq 0$ being generic, we will focus on operators that commute with both the hopping and the East-West term in the Hamiltonian.
- We identify the operators that commute with $\sigma_j^z, \sigma_{j+1}^z, (1 - \sigma_j^z)\sigma_{j+1}^x, (1 - \sigma_{j+1}^z)\sigma_j^x$ at a given position j . One can check that these also commute with $\sigma_j^+ \sigma_{j+1}^- + \sigma_j^- \sigma_{j+1}^+$.
- Finally, one intersects progressively the spaces of operators introduced above over the site index j . The result of this procedure, which can be obtained using induction on the length of the chain, gives precisely $\text{Span}\{\mathbb{1}, |\uparrow\rangle\langle\uparrow|\}$.

As a final remark, we point out that, for specific choices of the couplings, as for example $g = 0$ (where $\sum_j \sigma^z$ is conserved), additional symmetries can be present and the commutant algebra becomes larger: we dub that as a fine-tuning. In particular, since $\mathcal{C} \subseteq \ker \mathcal{L}$ (from the definition (8)) and a double degeneracy of

the zero-eigenvalue is observed at $g, J \neq 0$ (that is, $\ker \mathcal{L} = \text{Span}\{\mathbb{1}, |\uparrow\rangle\langle\uparrow|\}$), one safely concludes that $\mathcal{C} = \text{Span}\{\mathbb{1}, |\uparrow\rangle\langle\uparrow|\}$. Additional details are given in the SM.

Spectral properties of the Lindbladian — Here, we discuss the spectral properties of the Lindbladian in Eq. (1). We first, summarize the main steps to obtain the effective Markov generator W in Eq. (5), in the limit of small $g/\gamma, J/\gamma$. The method is based on second-order perturbation theory on the Lindbladian, and it has been employed in [17]:

- One first identifies the spectrum of the dissipator, found for $g, J = 0$ in Eq. (1). An explicit calculation shows that matrix elements of the form $|\sigma\rangle\langle\sigma'|$, with σ, σ' spin configurations in the z -direction, are eigenvectors and their eigenvalue is proportional to the number of mismatches between σ and σ' . In particular, in the absence of perturbation, the manifold of stationary states, associated with $\lambda = 0$, is generated by the diagonal elements $|\sigma\rangle\langle\sigma|$.
- For small $g, J \neq 0$, the large degeneracy of the Lindbladian is split and, at the lowest order, the effective couplings between unperturbed eigenvectors are given by virtual transitions onto unperturbed eigenspaces.
- Specifically, from the effective couplings between the diagonal elements $|\sigma\rangle\langle\sigma|$, one can identify an effective Lindbladian which describes the low spectrum of \mathcal{L} (and having the same matrix elements of $-W$). This allows us to reduce the complexity of diagonalizing a $4^L \times 4^L$ matrix, associated with \mathcal{L} , to the diagonalization of a $2^L \times 2^L$ matrix, corresponding to W , as far as the low-spectrum is concerned.

The explicit calculations to obtain the expression of W are straightforward but lengthy, and they are reported in the SM. As a byproduct, we perform a numerical check and we compare the spectrum of \mathcal{L} and that of $-W$ obtained via exact diagonalization using the open-source Python package QuSpin [53, 54]; in Fig. 5 we show the results for $L = 4$, with $[g, J, \gamma] = [0.5, 0.5, 100]$.

We now discuss the properties of the lowest energy states of the Markov generator above the ground state manifold. First, we observe that $W \geq 0$ and has $|\uparrow\rangle$ and $|\Rightarrow\rangle$ as exact eigenstates with vanishing energy (corresponding with the exceptional stationary state and the infinite temperature state, belonging to the kernel of the Lindbladian). Being this operator gapped, as shown numerically in Fig. 1, one expects that its first excited states correspond to domain-wall excitations, interpolating between the two ground states, at given momenta (a property that we found analytically for the simplified model \tilde{W} introduced in the main text): while this is

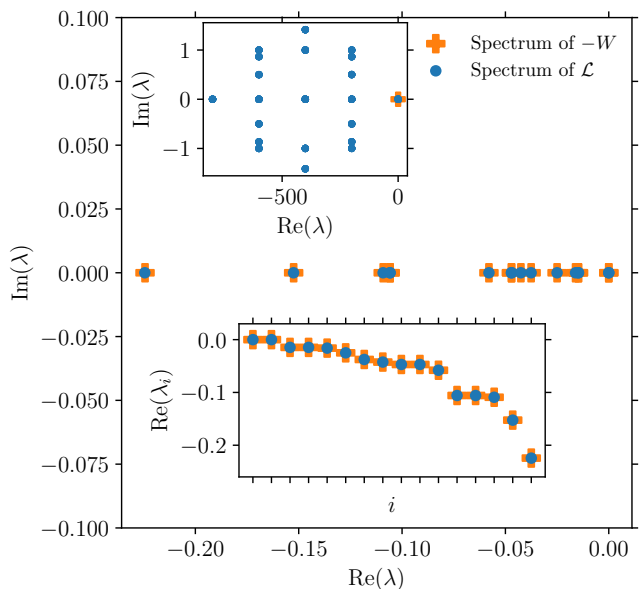


Figure 5. Comparison between the slow decaying modes of the Lindbladian \mathcal{L} and the spectrum of the effective Hamiltonian $-W$. The parameters are $[J, g, \gamma, L] = [0.5, 0.5, 100, 4]$. In the top inset, the full spectrum of \mathcal{L} is represented. In the bottom inset, we show the real part of the slow decaying modes labeled by the index i .

formally correct for infinite systems, carefulness is needed for finite systems, and the choice of boundary conditions plays a role. For instance, while a single domain wall can be present with open boundary conditions, only an even number of them can be hosted in the periodic chain: this is analogous to the properties of the spectrum of the quantum Ising chain [55]. As a consequence, the origin of the spectral gap is traced back to a 1- or 2-domain wall excitation with the lowest possible momenta (allowed from the quantization induced by the boundary conditions), for the open/periodic chain respectively. While the previous discussion refers to the Markov generator, we expect that similar properties holds for the Lindbladian. In particular, a discrepancy between the spectral gap with the two aforementioned boundary conditions is explicitly observed: in Fig. 6 we show the results with periodic boundary conditions, that have to be compared with those in Fig. 1

Details on the tensor-network numerical computations — Here, we give some details on the implementation of the tensor-network numerical simulations. We vectorize the density matrix ρ , as done in Refs. [56, 57]. In this representation, the Lindbladian \mathcal{L} becomes a linear operator. We represent the vectorized ρ as a matrix-product-state and \mathcal{L} as a matrix-product-operator. The time-evolution is performed using the Time-Dependent Variational Principle (TDVP) [41, 58, 59]. In this way, we are able to simulate chains of $L = 40$ sites up to time $t = 30$ for

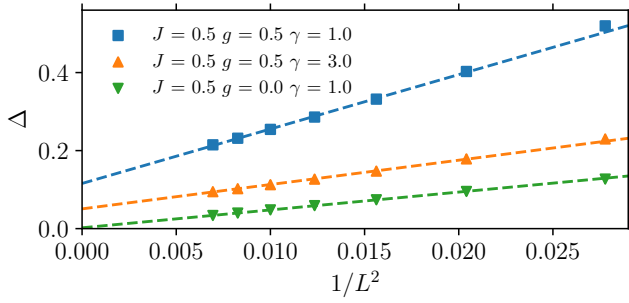


Figure 6. Lindbladian gap Δ as function of $1/L^2$ for $L \in \{6, \dots, 12\}$ and periodic boundary conditions.

$[J, g, \gamma] = [0.5, 0.5, 1]$. The bond-dimension, the number of sweeps and the time-step used in all this work are $\chi = 200$, $n_{\text{sweeps}} = 5$ and $\delta t = 0.1$ respectively.

On the exponential loss of coherence between \mathcal{S}_\uparrow and \mathcal{T}_\uparrow — We discuss here the exponential loss of coherence between $|\uparrow\rangle$ and the states orthogonal to it, expressed by the quantity $\eta(t)$ in Eq. (4). To study its behavior, we consider the evolution of $\langle \sigma | \rho(t) | \uparrow \rangle$, with $|\sigma\rangle \neq |\uparrow\rangle$. A simple calculation, starting from Eq. (1) gives

$$\frac{d}{dt} \langle \sigma | \rho(t) | \uparrow \rangle = \langle \sigma | -i[H, \rho(t)] + \gamma \sum_j (\sigma_j^z \rho(t) \sigma_j^z(t) - \rho(t)) | \uparrow \rangle. \quad (9)$$

Using $H|\uparrow\rangle = 0$ and $\sigma_j^z|\uparrow\rangle = |\uparrow\rangle$, we express

$$\frac{d}{dt} \langle \sigma | \rho(t) | \uparrow \rangle = - \sum_{|\sigma'\rangle \neq |\uparrow\rangle} \langle \sigma | K | \sigma' \rangle \langle \sigma' | \rho(t) | \uparrow \rangle \quad (10)$$

with $K = iH + \gamma \sum_j (1 - \sigma_j^z)$. In other words, the evolution of $\langle \sigma | \rho(t) | \uparrow \rangle$, seen as a column vector with entries parametrized by σ , is ruled by the matrix K . We observe that $K + K^\dagger = 2\gamma \sum_j (1 - \sigma_j^z)$, and therefore the eigenvalues of $K + K^\dagger$ are $\geq 4\gamma$ in the subspace orthogonal to $|\uparrow\rangle$. As a consequence, the entries of $\langle \sigma | \rho(t) | \uparrow \rangle$ are expected to decay exponentially with a rate proportional to γ . A quantitative estimate can be provided for the quantifier $\eta(t)$ and, after straightforward algebra, we obtain

$$-\frac{d}{dt} \eta(t) = \langle \uparrow | \rho(t) (K + K^\dagger) \rho(t) | \uparrow \rangle \geq 4\gamma \eta(t) \quad (11)$$

which implies $\eta(t) \leq e^{-4\gamma t} \eta(0)$.

[1] Michael V Berry, “Regular and irregular semiclassical wavefunctions,” *Journal of Physics A: Mathematical and General* **10**, 2083 (1977).
 [2] Josh M Deutsch, “Quantum statistical mechanics in a closed system,” *Phys. Rev. A* **43**, 2046 (1991).

[3] Mark Srednicki, “The approach to thermal equilibrium in quantized chaotic systems,” *Journal of Physics A: Mathematical and General* **32**, 1163 (1999).
 [4] Luca D’Alessio, Yariv Kafri, Anatoli Polkovnikov, and Marcos Rigol, “From quantum chaos and eigenstate thermalization to statistical mechanics and thermodynamics,” *Advances in Physics* **65**, 239–362 (2016).
 [5] Silvia Pappalardi, Laura Foini, and Jorge Kurchan, “Eigenstate thermalization hypothesis and free probability,” *Phys. Rev. Lett.* **129** (2022).
 [6] Hannes Bernien, Sylvain Schwartz, A Keesling, H Levine, Ahmed Omran, Hannes Pichler, Soonwon Choi, A. S. Zibrov, Manuel Endres, Markus Greiner, Vladan Vuletić, and Mikhail D. Lukin, “Probing many-body dynamics on a 51-atom quantum simulator,” *Nature* **551**, 579–584 (2017).
 [7] C. J. Turner, A. A. Michailidis, D. A. Abanin, M. Serbyn, and Z. Papić, “Weak ergodicity breaking from quantum many-body scars,” *Nature Physics* **14**, 745–749 (2018).
 [8] Maksym Serbyn, Dmitry A. Abanin, and Zlatko Papić, “Quantum many-body scars and weak breaking of ergodicity,” *Nature Physics* **17**, 675–685 (2021).
 [9] Sanjay Moudgalya, B Andrei Bernevig, and Nicolas Regnault, “Quantum many-body scars and Hilbert space fragmentation: a review of exact results,” *Reports on Progress in Physics* **85**, 086501 (2022).
 [10] Anushya Chandran, Thomas Iadecola, Vedika Khemani, and Roderich Moessner, “Quantum many-body scars: A quasiparticle perspective,” *Annual Rev. of Cond. Matt. Phys.* **14**, 443–469 (2023).
 [11] Rosario Fazio, Jonathan Keeling, Leonardo Mazza, and Marco Schiro, “Many-body open quantum systems,” (2024), arXiv:2409.10300 [quant-ph].
 [12] Lukas M. Sieberer, Michael Buchhold, Jamir Marino, and Sebastian Diehl, “Universality in driven open quantum matter,” (2023), arXiv:2312.03073 [cond-mat.stat-mech].
 [13] E. M. Kessler, G. Giedke, A. Imamoglu, S. F. Yelin, M. D. Lukin, and J. I. Cirac, “Dissipative phase transition in a central spin system,” *Phys. Rev. A* **86**, 012116 (2012).
 [14] Fabrizio Minganti, Alberto Biella, Nicola Bartolo, and Cristiano Ciuti, “Spectral theory of Liouvillians for dissipative phase transitions,” *Phys. Rev. A* **98**, 042118 (2018).
 [15] Dario Poletti, Jean-Sébastien Bernier, Antoine Georges, and Corinna Kollath, “Interaction-induced impeding of decoherence and anomalous diffusion,” *Phys. Rev. Lett.* **109**, 045302 (2012).
 [16] Dario Poletti, Peter Barmettler, Antoine Georges, and Corinna Kollath, “Emergence of glasslike dynamics for dissipative and strongly interacting bosons,” *Phys. Rev. Lett.* **111**, 195301 (2013).
 [17] Zi Cai and Thomas Barthel, “Algebraic versus exponential decoherence in dissipative many-particle systems,” *Phys. Rev. Lett.* **111**, 150403 (2013).
 [18] Raphaël Bouganne, Manel Bosch Aguilera, Alexis Ghermaoui, Jérôme Beugnon, and Fabrice Gerbier, “Anomalous decay of coherence in a dissipative many-body system,” *Nature Physics* **16**, 21–25 (2019).
 [19] D. Wellnitz, G. Preisser, V. Alba, J. Dubail, and J. Schachenmayer, “Rise and fall, and slow rise again, of operator entanglement under dephasing,” *Phys. Rev. Lett.* **129**, 170401 (2022).

- [20] Yahui Li, Pablo Sala, and Frank Pollmann, “Hilbert space fragmentation in open quantum systems,” *Phys. Rev. Res.* **5**, 043239 (2023).
- [21] Yahui Li, Frank Pollmann, Nicholas Read, and Pablo Sala, “Highly-entangled stationary states from strong symmetries,” (2024), arXiv:2406.08567 [quant-ph].
- [22] Berislav Buča and Tomaž Prosen, “A note on symmetry reductions of the lindblad equation: transport in constrained open spin chains,” *New Journal of Physics* **14**, 073007 (2012).
- [23] Victor V. Albert and Liang Jiang, “Symmetries and conserved quantities in lindblad master equations,” *Phys. Rev. A* **89**, 022118 (2014).
- [24] Marko Žnidarič, “Relaxation times of dissipative many-body quantum systems,” *Phys. Rev. E* **92**, 042143 (2015).
- [25] Takashi Mori and Tatsuhiko Shirai, “Resolving a discrepancy between liouvillian gap and relaxation time in boundary-dissipated quantum many-body systems,” *Phys. Rev. Lett.* **125**, 230604 (2020).
- [26] Taiki Haga, Masaya Nakagawa, Ryusuke Hamazaki, and Masahito Ueda, “Liouvillian skin effect: Slowing down of relaxation processes without gap closing,” *Phys. Rev. Lett.* **127**, 070402 (2021).
- [27] Tibor Rakovszky, Sarang Gopalakrishnan, and Curt von Keyserlingk, “Defining stable phases of open quantum systems,” *Phys. Rev. X* **14**, 041031 (2024).
- [28] Nicola Pancotti, Giacomo Giudice, J. Ignacio Cirac, Juan P. Garrahan, and Mari Carmen Bañuls, “Quantum east model: Localization, nonthermal eigenstates, and slow dynamics,” *Phys. Rev. X* **10**, 021051 (2020).
- [29] Saverio Bocini and Maurizio Fagotti, “Growing Schrödinger’s cat states by local unitary time evolution of product states,” *Phys. Rev. Res.* **6**, 033108 (2024).
- [30] Daniel Lidar, “Review of decoherence free subspaces, noiseless subsystems, and dynamical decoupling,” *Advances in Chemical Physics* **154** (2012), 10.1002/9781118742631.ch11.
- [31] J.R. Johansson, P.D. Nation, and Franco Nori, “Qutip: An open-source python framework for the dynamics of open quantum systems,” *Computer Physics Communications* **183**, 1760–1772 (2012).
- [32] J.R. Johansson, P.D. Nation, and Franco Nori, “Qutip 2: A python framework for the dynamics of open quantum systems,” *Computer Physics Communications* **184**, 1234–1240 (2013).
- [33] Sanjay Moudgalya and Olexei I. Motrunich, “Hilbert space fragmentation and commutant algebras,” *Phys. Rev. X* **12**, 011050 (2022).
- [34] Sanjay Moudgalya and Olexei I. Motrunich, “From symmetries to commutant algebras in standard Hamiltonians,” *Annals of Physics* **455**, 169384 (2023).
- [35] Sanjay Moudgalya and Olexei I. Motrunich, “Exhaustive characterization of quantum many-body scars using commutant algebras,” (2023), arXiv:2209.03377 [cond-mat.str-el].
- [36] “See the supplemental material.”
- [37] We remark that, at $g = 0$ the degeneracy of the eigenvalue $\lambda = 0$ is enhanced, due to the $U(1)$ symmetry associated with the conservation of the magnetization along the z -axis.
- [38] Matthew Fishman, Steven R. White, and E. Miles Stoudenmire, “The ITensor Software Library for Tensor Network Calculations,” *SciPost Phys. Codebases* , 4 (2022).
- [39] Matthew Fishman, Steven R. White, and E. Miles Stoudenmire, “Codebase release 0.3 for ITensor,” *SciPost Phys. Codebases* , 4–r0.3 (2022).
- [40] Mingru Yang and Steven R. White, “Time-dependent variational principle with ancillary Krylov subspace,” *Phys. Rev. B* **102**, 094315 (2020).
- [41] Jutho Haegeman, J. Ignacio Cirac, Tobias J. Osborne, Iztok Pizorn, Henri Verschelde, and Frank Verstraete, “Time-dependent variational principle for quantum lattices,” *Phys. Rev. Lett.* **107**, 070601 (2011).
- [42] He-Ran Wang, Dong Yuan, Shun-Yao Zhang, Zhong Wang, Dong-Ling Deng, and L.-M. Duan, “Embedding quantum many-body scars into decoherence-free subspaces,” *Phys. Rev. Lett.* **132**, 150401 (2024).
- [43] Marius de Leeuw, Chiara Paletta, Balázs Pozsgay, and Eric Vernier, “Hidden quasiloccal charges and Gibbs ensemble in a Lindblad system,” *Phys. Rev. B* **109**, 054311 (2024).
- [44] Víctor Fernández-Hurtado, Jordi Mur-Petit, Juan José García-Ripoll, and Rafael A Molina, “Lattice scars: surviving in an open discrete billiard,” *New Journal of Physics* **16**, 035005 (2014).
- [45] Berislav Buča, Joseph Tindall, and Dieter Jaksch, “Non-stationary coherent quantum many-body dynamics through dissipation,” *Nature Communications* **10**, 1730 (2019).
- [46] Qianqian Chen, Shuai A. Chen, and Zheng Zhu, “Weak ergodicity breaking in non-Hermitian many-body systems,” *SciPost Phys.* **15**, 052 (2023).
- [47] Adam Nahum, Jonathan Ruhman, Sagar Vijay, and Jeongwan Haah, “Quantum entanglement growth under random unitary dynamics,” *Phys. Rev. X* **7**, 031016 (2017).
- [48] Tianci Zhou and Adam Nahum, “Entanglement membrane in chaotic many-body systems,” *Phys. Rev. X* **10**, 031066 (2020).
- [49] Masao Doi, “Stochastic theory of diffusion-controlled reaction,” *Journal of Physics A: Mathematical and General* **9**, 1479 (1976).
- [50] Masao Doi, “Second quantization representation for classical many-particle system,” *Journal of Physics A: Mathematical and General* **9**, 1465 (1976).
- [51] Federico Gerbino, Igor Lesanovsky, and Gabriele Peretto, “Large-scale universality in quantum reaction-diffusion from Keldysh field theory,” *Phys. Rev. B* **109**, L220304 (2024).
- [52] Alice Marché, Hironobu Yoshida, Alberto Nardin, Hosho Katsura, and Leonardo Mazza, “Universality and two-body losses: Lessons from the effective non-hermitian dynamics of two particles,” *Phys. Rev. A* **110**, 033321 (2024).
- [53] Phillip Weinberg and Marin Bukov, “QuSpin: a Python package for dynamics and exact diagonalisation of quantum many body systems part I: spin chains,” *SciPost Phys.* **2**, 003 (2017).
- [54] Phillip Weinberg and Marin Bukov, “QuSpin: a Python package for dynamics and exact diagonalisation of quantum many body systems. Part II: bosons, fermions and higher spins,” *SciPost Phys.* **7**, 020 (2019).
- [55] Subir Sachdev, “Quantum phase transitions,” *Physics world* **12**, 33 (1999).
- [56] F. Verstraete, J. J. García-Ripoll, and J. I. Cirac, “Matrix product density operators: Simulation of finite-

- temperature and dissipative systems,” *Phys. Rev. Lett.* **93**, 207204 (2004).
- [57] Jian Cui, J. Ignacio Cirac, and Mari Carmen Bañuls, “Variational matrix product operators for the steady state of dissipative quantum systems,” *Phys. Rev. Lett.* **114**, 220601 (2015).
- [58] Sebastian Paeckel, Thomas Köhler, Andreas Swoboda, Salvatore R. Manmana, Ulrich Schollwöck, and Claudius Hubig, “Time-evolution methods for matrix-product states,” *Annals of Physics* **411**, 167998 (2019).
- [59] Jutho Haegeman, Christian Lubich, Ivan Oseledets, Bart Vandereycken, and Frank Verstraete, “Unifying time evolution and optimization with matrix product states,” *Phys. Rev. B* **94**, 165116 (2016).
- [60] Here, we did not consider the commutant coming from the hopping term in Eq. (2). The reason is that its (large) commutant contains already $\mathbb{1}$ and $|\uparrow\rangle\langle\uparrow|$: therefore we do not get any additional information from its intersection with (17).
- [61] A technical point is needed here. Given $\mathcal{A}_1 \subseteq \text{End}(\mathcal{H}_1)$, one can always construct the embedding $\mathcal{A}_1 \otimes \mathbb{1}_{\mathcal{H}_2} \subseteq \text{End}(\mathcal{H}_1 \otimes \mathcal{H}_2)$ for any other Hilbert space \mathcal{H}_2 . The commutant of the associated embedding is $\mathcal{C}[\mathcal{A}_1 \otimes \mathbb{1}_{\mathcal{H}_2}] = \mathcal{C}[\mathcal{A}_1] \otimes \text{End}(\mathcal{H}_2)$.
- [62] Hal Tasaki, *Physics and mathematics of quantum many-body systems*, Vol. 66 (Springer, 2020).
- [63] Stefan Knabe, “Energy gaps and elementary excitations for certain VBS-quantum antiferromagnets,” *Journal of Statistical Physics* **52**, 627–638 (1988).

Supplemental Material:
“Exceptional stationary state in a dephasing many-body open quantum system”

Commutant algebra

In this section, we discuss the properties of the commutant algebra (reviewed in [33, 34]) associated with the model in Eq. (1). We will prove that the commutant algebra of (1) is generated by the two stationary states $\mathbb{1}$ and $|\uparrow\rangle\langle\uparrow|$.

Before entering the calculations, we briefly review some basic definitions and properties of algebras and their commutants. Given a set of operators $\{\mathcal{O}_j\}$, we denote the (C^* -)algebra they generate by $\text{Alg}(\{\mathcal{O}_j\})$: this is a vector space of operators that is closed under products and the adjoint operation \dagger and it contains the identity $\mathbb{1}$. For any algebra of operators \mathcal{A} , we introduce its commutant

$$\mathcal{C}[\mathcal{A}] \equiv \{c \mid [c, a] = 0 \ \forall a \in \mathcal{A}\}. \quad (12)$$

Given two algebras $\mathcal{A}_1, \mathcal{A}_2$, we consider $\mathcal{A}_1 \cdot \mathcal{A}_2 \equiv \text{Alg}(\{\mathcal{A}_1, \mathcal{A}_2\})$ the algebra generated by their products: one can show from the definition (12) that

$$\mathcal{C}[\mathcal{A}_1 \cdot \mathcal{A}_2] = \mathcal{C}[\mathcal{A}_1] \cap \mathcal{C}[\mathcal{A}_2]. \quad (13)$$

In other words, the commutant of $\mathcal{A}_1 \cdot \mathcal{A}_2$ contains the operators that commute with both \mathcal{A}_1 and \mathcal{A}_2 . Lastly, we recall that, in the context of open quantum systems, it is convenient to associate the commutant algebra with the local terms of Lindbladians, that is

$$\mathcal{C} \equiv \mathcal{C}[\text{Alg}\{h_j, L_j\}_j]. \quad (14)$$

Here, h_j is the Hamiltonian density, satisfying $H = \sum_j h_j$, and L_j are the jump operators entering the dissipative term of the Lindbladian. In particular, from (1) and (14), one gets $\mathcal{L}[\mathcal{C}] = 0$, meaning that $\mathcal{C} \subseteq \text{Ker}(\mathcal{L})$ and the elements of the commutant algebra generate stationary states.

We now focus on the model (1) and, with a direct calculation, we show directly

$$\text{Span}\{\mathbb{1}, |\uparrow\rangle\langle\uparrow|\} \subseteq \mathcal{C}, \quad (15)$$

since both the stationary state and the scar are annihilated by each term of the Lindbladian. In the remaining part of this section, we will prove that equality holds in Eq. (15). To do so, we follow this strategy:

- We identify the commutant algebra associated with operators inserted on a given site $j = j_0$. Specifically, since the Hamiltonian density contains 2-site operators, the associated operators have support on j_0 and $j_0 + 1$.
- We intersect it with the commutant algebra associated with insertions at $j = j_0 + 1$.
- We progressively reiterate this process, by intersecting commutant algebras at any position j .

Without loss of generality, we consider $j_0 = 1$, restricting the analysis on the operators acting on $j = 1, 2$ (isomorphic to $\text{End}(\mathbb{C}^2 \otimes \mathbb{C}^2)$). Here, straightforward linear algebra shows that

$$\begin{aligned} \mathcal{C}[\text{Alg}\{\sigma^z \otimes 1, 1 \otimes \sigma^z\}] &= \text{Span}\{|\uparrow\uparrow\rangle\langle\uparrow\uparrow|, |\uparrow\downarrow\rangle\langle\uparrow\downarrow|, |\downarrow\uparrow\rangle\langle\downarrow\uparrow|, |\downarrow\downarrow\rangle\langle\downarrow\downarrow|\}, \\ \mathcal{C}[\text{Alg}\{(1 - \sigma^z) \otimes \sigma^x\}] &= (|\uparrow\rangle\langle\uparrow| \otimes \text{End}(\mathbb{C}^2)) \oplus (|\downarrow\rangle\langle\downarrow| \otimes \text{Span}\{|\rightarrow\rangle\langle\rightarrow|, |\leftarrow\rangle\langle\leftarrow|\}), \\ \mathcal{C}[\text{Alg}\{\sigma^x \otimes (1 - \sigma^z)\}] &= (\text{End}(\mathbb{C}^2) \otimes |\uparrow\rangle\langle\uparrow|) \oplus (\text{Span}\{|\rightarrow\rangle\langle\rightarrow|, |\leftarrow\rangle\langle\leftarrow|\} \otimes |\downarrow\rangle\langle\downarrow|). \end{aligned} \quad (16)$$

We intersect the three spaces above and the result is

$$\mathcal{C}[\text{Alg}\{\sigma^z \otimes 1, 1 \otimes \sigma^z, (1 - \sigma^z) \otimes \sigma^x, \sigma^x \otimes (1 - \sigma^z)\}] = \text{Span}\{\mathbb{1}, |\uparrow\uparrow\rangle\langle\uparrow\uparrow|\}; \quad (17)$$

this is explicitly the commutant [60] for a chain of length $L = 2$. We now consider the operators with support on $j = 1, 2, 3$ as elements of $\text{End}((\mathbb{C}^2)^{\otimes 3})$, coming from the insertions at $j = 1, 2$. We embed [61] the commutant (17) in this space, and similarly the one associated with $j = 2$: we intersect them, and, after simple calculations, we obtain $\text{Span}\{\mathbb{1}, |\uparrow\uparrow\rangle\langle\uparrow\uparrow|\}$. We repeat this procedure and, by induction, we eventually find the equality in Eq. (15)

Effective Lindbladian

Here, we give details regarding the computation of the effective Markov generator W in (5), obtained using perturbation theory. It is convenient to consider the doubled Hilbert space $\mathcal{H} \otimes \mathcal{H}^*$, with \mathcal{H} the Hilbert space of the chain and \mathcal{H}^* its dual. In particular, we regard ρ as a vector of $\mathcal{H} \otimes \mathcal{H}^*$ and \mathcal{L} as an operator acting on it, that is $\mathcal{L} \in \text{End}(\mathcal{H} \otimes \mathcal{H}^*)$. In this formalism, we express the Lindbladian in Eq. (1) as

$$\mathcal{L} = -i(H \otimes 1^* - 1 \otimes H^*) + \sum_j [L_j \otimes (L_j^\dagger)^* - \frac{1}{2}(L_j^\dagger L_j) \otimes 1^* - \frac{1}{2}1 \otimes (L_j^\dagger L_j)^*], \quad (18)$$

where the action of $\mathcal{O}_1 \otimes \mathcal{O}_2^* \in \text{End}(\mathcal{H} \otimes \mathcal{H}^*)$ on ρ is $(\mathcal{O}_1 \otimes \mathcal{O}_2^*)\rho = \mathcal{O}_1\rho\mathcal{O}_2$. The unperturbed Lindbladian (obtained for $H = 0$) is

$$\mathcal{L}^{(0)} := -2\gamma \sum_j \frac{1 - \sigma_j^z \otimes (\sigma_j^z)^*}{2}. \quad (19)$$

We identify its eigenspaces

$$V_n = \text{Span}\{|\sigma\rangle\langle\sigma'|\}, \quad (20)$$

where σ, σ' are spin-configurations in the z -basis which differ by n spins ($n = 0, \dots, L$), with eigenvalue $\lambda_n \equiv -2\gamma n$. We denote the associated spectral projector by Π_j . We apply second-order perturbation, treating perturbatively the commutator $-i[H, \cdot]$. We do so, and we identify an effective Lindbladian \mathcal{L}_{eff} acting on V_0

$$\begin{aligned} \mathcal{L}_{\text{eff}} \simeq & (-i)^2 \sum_{n \neq 0} \Pi_0(H \otimes 1^* - 1 \otimes H^*) \Pi_n \frac{1}{\lambda_0 - \lambda_n} \Pi_n(H \otimes 1^* - 1 \otimes H^*) \Pi_0 = \\ & -2 \sum_{n \neq 0} \frac{\Pi_0(H \otimes 1^*) \Pi_n(H \otimes 1^*) \Pi_0}{\lambda_0 - \lambda_n} + 2 \sum_{n \neq 0} \frac{\Pi_0(H \otimes 1^*) \Pi_n(1 \otimes H^*) \Pi_0}{\lambda_0 - \lambda_n}. \end{aligned} \quad (21)$$

It is worth observing that, for the specific Hamiltonian H in Eq. (2), $(1 \otimes H^*)$, $(H \otimes 1^*)$ connects V_0 to V_n for $n = 1$ (through the East-West term) and $n = 2$ (via the hopping term) only. Before entering the calculation of (21), which is lengthy, albeit straightforward, we remind that the validity of this approach is justified whenever the spectral gap above V_0 persists in the presence of the perturbation ($g, J \neq 0$): this might be an issue in the thermodynamic limit $L \rightarrow \infty$, and only focus in the regime of g, J at fixed L .

Following Ref. [17], we characterize \mathcal{L}_{eff} through its action over $|\sigma\rangle\langle\sigma|$ and via the equivalence $\mathcal{L}_{\text{eff}} \leftrightarrow -W$. We consider the East-West term in Eq. (2) first, which generates terms $\propto g^2/\gamma$ in \mathcal{L}_{eff} . We focus on the contributions appearing in the first term in the r.h.s. of (21). We compute them obtaining

- $\left[\sigma_j^x \left(\frac{1 - \sigma_{j+1}^z}{2}\right) \otimes 1^*\right] \Pi_1 \left[\sigma_j^x \left(\frac{1 - \sigma_{j+1}^z}{2}\right) \otimes 1^*\right] \cdot |\sigma\rangle\langle\sigma| = \left[\left(\frac{1 - \sigma_{j+1}^z}{2}\right) \otimes 1^*\right] \cdot |\sigma\rangle\langle\sigma|$. A similar term from the exchange $j \leftrightarrow j+1$ appears. These generate a term $4 \frac{(2g)^2}{2\gamma} \sum_j \frac{1 - \sigma_{j+1}^z}{2}$ in W .
- $\left[\sigma_j^x \left(\frac{1 - \sigma_{j+1}^z}{2}\right) \otimes 1^*\right] \Pi_1 \left[\sigma_j^x \left(\frac{1 - \sigma_{j-1}^z}{2}\right) \otimes 1^*\right] \cdot |\sigma\rangle\langle\sigma| = \left[\left(\frac{1 - \sigma_j^z}{2}\right) \left(\frac{1 - \sigma_{j+1}^z}{2}\right) \otimes 1^*\right] \cdot |\sigma\rangle\langle\sigma|$. A similar term with $j+1 \leftrightarrow j-1, j \leftrightarrow j$ gives the same contribution; finally, we obtain a term $4 \frac{(2g)^2}{2\gamma} \sum_j \frac{1 - \sigma_{j-1}^z}{2} \frac{1 - \sigma_{j+1}^z}{2}$ for W .

In the second term in Eq. (21), these contributions appear:

- $\left[\sigma_j^x \left(\frac{1 - \sigma_{j+1}^z}{2}\right) \otimes 1^*\right] \Pi_1 \left[1 \otimes \left(\sigma_j^x \left(\frac{1 - \sigma_{j+1}^z}{2}\right)\right)^*\right] \cdot |\sigma\rangle\langle\sigma| = \left[\left(\frac{1 - \sigma_{j+1}^z}{2}\right) \sigma_j^x \otimes (\sigma_j^x)^*\right] \cdot |\sigma\rangle\langle\sigma|$. A similar term from the exchange $j \leftrightarrow j+1$ appears. These generate a term $-2 \frac{(2g)^2}{2\gamma} \sum_j \frac{1 - \sigma_j^z}{2} (\sigma_{j+1}^x + \sigma_{j-1}^x)$ in W .
- $\left[\sigma_j^x \left(\frac{1 - \sigma_{j+1}^z}{2}\right) \otimes 1^*\right] \Pi_1 \left[1 \otimes \left(\sigma_j^x \left(\frac{1 - \sigma_{j-1}^z}{2}\right)\right)^*\right] \cdot |\sigma\rangle\langle\sigma| = \left[\left(\frac{1 - \sigma_{j-1}^z}{2}\right) \left(\frac{1 - \sigma_{j+1}^z}{2}\right) \sigma_j^x \otimes (\sigma_j^x)^*\right] \cdot |\sigma\rangle\langle\sigma|$. A similar term, with $j+1 \leftrightarrow j-1, j \leftrightarrow j$ exchanged in the previous formula, gives the same contribution; finally, we obtain the term $-4 \frac{(2g)^2}{2\gamma} \sum_j \frac{1 - \sigma_{j-1}^z}{2} \sigma_j^x \frac{1 - \sigma_{j+1}^z}{2}$ for W .

For the hopping term in Eq. (2), which gives a contribution proportional to J^2/γ for W , the calculations are reported below. We observe, that $\sigma_j^+ \sigma_{j+1}^- + \sigma_j^- \sigma_{j+1}^+ = \sigma_j^x \sigma_{j+1}^x \left(\frac{1 - \sigma_j^z \sigma_{j+1}^z}{2} \right)$, and it acts in the z basis by flipping the two spins at j and $j+1$ only when they are different. Thus, from the first term in (21), we obtain

- $[(\sigma_j^+ \sigma_{j+1}^- + \sigma_j^- \sigma_{j+1}^+) \otimes 1^*] \Pi_2 [(\sigma_j^+ \sigma_{j+1}^- + \sigma_j^- \sigma_{j+1}^+) \otimes 1^*] \cdot |\sigma\rangle\langle\sigma| = \left[\frac{1 - \sigma_j^z \sigma_{j+1}^z}{2} \otimes 1^* \right] \cdot |\sigma\rangle\langle\sigma|$. This contributes as $\frac{J^2}{4\gamma} \sum_j \frac{1 - \sigma_j^z \sigma_{j+1}^z}{2}$ to W .

Similarly, from the second term of (21):

- $[(\sigma_j^+ \sigma_{j+1}^- + \sigma_j^- \sigma_{j+1}^+) \otimes 1^*] \Pi_2 [1 \otimes (\sigma_j^+ \sigma_{j+1}^- + \sigma_j^- \sigma_{j+1}^+)^*] \cdot |\sigma\rangle\langle\sigma| = \left[\frac{1 - \sigma_j^z \sigma_{j+1}^z}{2} \sigma_j^x \sigma_{j+1}^x \otimes (\sigma_j^x \sigma_{j+1}^x)^* \right] \cdot |\sigma\rangle\langle\sigma|$. This contributes as $-\frac{J^2}{4\gamma} \sum_j \sigma_j^x \sigma_{j+1}^x \frac{1 - \sigma_j^z \sigma_{j+1}^z}{2} = -\frac{J^2}{4\gamma} \sum_j (\sigma_j^x \sigma_{j+1}^x + \sigma_j^y \sigma_{j+1}^y)$ to W .

Putting everything together, we arrive at the expression in Eq. (5). As a byproduct of the validity of the result, we easily check $\langle \Rightarrow | W = 0$: such a property corresponds, in the Doi-Peliti formalism, to the conservation of the probability. While this is required for a well-defined Markov chain, it is not completely obvious that this property holds consistently through the perturbative analysis.

Properties of the Markov generator \tilde{W}

In this section, we discuss the properties of the operator \tilde{W} defined in the main text. We write $\tilde{W} = \sum_j \tilde{w}_j$, with \tilde{w}_j acting on j and $j+1$ whose matrix representation (in the basis $\{|\uparrow\uparrow\rangle, |\uparrow\downarrow\rangle, |\downarrow\uparrow\rangle, |\downarrow\downarrow\rangle\}$) is

$$\tilde{w}_j = \frac{1}{3} \begin{pmatrix} 0 & 0 & 0 & 0 \\ 0 & 2 & -1 & -1 \\ 0 & -1 & 2 & -1 \\ 0 & -1 & -1 & 2 \end{pmatrix}. \quad (22)$$

In particular, the entries are chosen so that the configuration $|\uparrow\uparrow\rangle$ is stationary, while the other three mix among each other with equal rates. This allows us to identify two sectors, namely $\text{Span}\{|\uparrow\uparrow\rangle\}$ and its orthogonal complement: the first is associated with the stationary state $|\uparrow\uparrow\rangle$, while the second is associated with

$$\frac{1}{2^L - 1} \left(\sum_{\sigma} |\sigma\rangle - |\uparrow\uparrow\rangle \right) = \frac{2^L}{2^L - 1} |\bullet\rangle - \frac{1}{2^L - 1} |\uparrow\uparrow\rangle, \quad (23)$$

that is the infinite temperature state $|\bullet\rangle$ with the contribution of $|\uparrow\uparrow\rangle$ being subtracted; this subtraction does not play a role in the infinite volume limit $L \rightarrow \infty$, since the discrepancy with $|\bullet\rangle$ is exponentially small in L .

No additional stationary states are present at any finite size L , and $\ker \tilde{W} = \text{Span}\{|\uparrow\uparrow\rangle, |\Rightarrow\rangle\}$: to prove it rigorously, we observe that \tilde{w}_j are frustration-free generators, meaning that $\tilde{w}_j \geq 0$. Consequently [62], the kernel, spanned by the stationary states, is

$$\ker \tilde{W} = \bigcap_j \ker \tilde{w}_j. \quad (24)$$

One can intersect the kernels of \tilde{w}_j explicitly, obtaining the final result via Eq. (24). We point out that the same technique can be applied for W in Eq. (5), which gives $\ker W = \text{Span}\{|\uparrow\uparrow\rangle, |\Rightarrow\rangle\}$.

The analysis of the spectral gap of \tilde{W} is less straightforward. Nonetheless, for the specific choice of the generators \tilde{w}_j , that are 2-site projectors (satisfying $(\tilde{w}_j)^2 = \tilde{w}_j$) it is possible to use a technique introduced by Knabe in Ref. [63], to prove the existence of a finite spectral gap: we briefly review it here. The method boils down to analyzing the energy spectrum at finite size in open boundary conditions; in particular, we introduce

$$\tilde{W}_L = \sum_{j=1}^{L-1} \tilde{w}_j, \quad (25)$$

that acts non-trivially on the first L sites, and, given its spectral gap E_L , one can show [63]

$$\liminf_{L' \rightarrow \infty} E_{L'} \geq \frac{L-1}{L-2} \left(E_L - \frac{1}{L-1} \right) \quad \forall L \geq 3. \quad (26)$$

This gives an explicit lower bound to the spectral gap, that can be computed numerically for small system sizes (for example $L = 3, 4$). In our specific case, we find, by exact diagonalization

$$\frac{L-1}{L-2} \left(E_L - \frac{1}{L-1} \right) \simeq 0.05719, \quad L = 3, \quad (27)$$

that guarantees the finiteness of the spectral gap in the infinite volume limit.

In the rest of this section, we study the (quantum) single-particle problem associated with the propagation of a kink, and we relate it to the spectral gap of \tilde{W} . We introduce the states

$$|x\rangle_q \equiv |\rightarrow \cdots \rightarrow \underset{x}{\rightarrow} \uparrow \uparrow \cdots \uparrow\rangle, \quad (28)$$

which differ from $|x\rangle$, introduced in the main text, by a (x -dependent) proportionality constant. From Eq. (22), we find that

$$\tilde{w}_j |\rightarrow \uparrow\rangle_{j,j+1} = -\frac{\sqrt{2}}{3} |\rightarrow \rightarrow\rangle_{j,j+1} - \frac{\sqrt{2}}{3} |\uparrow \uparrow\rangle_{j,j+1} + |\rightarrow \uparrow\rangle_{j,j+1}, \quad \tilde{w}_j |\uparrow \uparrow\rangle_{j,j+1} = \tilde{w}_j |\rightarrow \rightarrow\rangle_{j,j+1} = 0, \quad (29)$$

implying

$$\tilde{W} |x\rangle_q = -\frac{\sqrt{2}}{3} \left(|x-1\rangle_q + |x+1\rangle_q \right) + |x\rangle_q. \quad (30)$$

The associated quantum dynamics can be solved exactly as

$$e^{-i\tilde{W}t} |x=0\rangle_q = \sum_x \psi(x,t) |x\rangle_q, \quad \psi(x,t) = \int_{-\pi}^{\pi} \frac{dk}{2\pi} e^{ikx - iE(k)t} \quad (31)$$

and the single-particle dispersion $E(k)$ is

$$E(k) = 1 - \frac{2\sqrt{2}}{3} \cos k > 0. \quad (32)$$

Interestingly, the lowest energy of the band is $E(k=0) \simeq 0.05719$ which is exactly the lower bound of the gap obtained in (27) via the Knabe's method: thus, we identify $E(k=0)$ as the spectral gap of the model and the one-kink band as the low energy spectrum.